This is the accepted manuscript made available via CHORUS. The article has been published as:

Phase Competition in the Palmer-Chalker XY Pyrochlore Er_{2}Pt_{2}O_{7}

A. M. Hallas, J. Gaudet, N. P. Butch, Guangyong Xu, M. Tachibana, C. R. Wiebe, G. M. Luke, and B. D. Gaulin

Phys. Rev. Lett. **119**, 187201 — Published 30 October 2017

DOI: 10.1103/PhysRevLett.119.187201

Phase Competition in the Palmer-Chalker XY Pyrochlore $Er_2Pt_2O_7$

A. M. Hallas,[1] J. Gaudet,[1] N. P. Butch,[2] Guangyong Xu,[2]
M. Tachibana,[3] C. R. Wiebe,[1,4,5] G. M. Luke,[1,5] and B. D. Gaulin[1,5,6]

[1]*Department of Physics and Astronomy, McMaster University, Hamilton, ON, L8S 4M1, Canada*
[2]*Center for Neutron Research, National Institute of Standards and Technology, MS 6100 Gaithersburg, Maryland 20899, USA*
[3]*National Institute for Materials Science, 1-1 Namiki, Tsukuba 305-0044, Ibaraki, Japan*
[4]*Department of Chemistry, University of Winnipeg, Winnipeg, MB, R3B 2E9 Canada*
[5]*Canadian Institute for Advanced Research, 180 Dundas St. W., Toronto, ON, M5G 1Z7, Canada*
[6]*Brockhouse Institute for Materials Research, Hamilton, ON L8S 4M1 Canada*

(Dated: September 25, 2017)

We report neutron scattering measurements on $Er_2Pt_2O_7$, a new addition to the XY family of frustrated pyrochlore magnets. Symmetry analysis of our elastic scattering data shows that $Er_2Pt_2O_7$ orders into the $k = 0$, Γ_7 magnetic structure (the Palmer-Chalker state), at $T_N = 0.38$ K. This contrasts with its sister XY pyrochlore antiferromagnets $Er_2Ti_2O_7$ and $Er_2Ge_2O_7$, both of which order into Γ_5 magnetic structures at much higher temperatures, $T_N = 1.2$ K and 1.4 K, respectively. In this temperature range, the magnetic heat capacity of $Er_2Pt_2O_7$ contains a broad anomaly centered at $T^* = 1.5$ K. Our inelastic neutron scattering measurements reveal that this broad heat capacity anomaly sets the temperature scale for strong short-range spin fluctuations. Below $T_N = 0.38$ K, $Er_2Pt_2O_7$ displays a gapped spin wave spectrum with an intense, flat band of excitations at lower energy and a weak, diffusive band of excitations at higher energy. The flat band is well-described by classical spin wave calculations, but these calculations also predict sharp dispersive branches at higher energy, a striking discrepancy with the experimental data. This, in concert with the strong suppression of T_N, is attributable to enhanced quantum fluctuations due to phase competition between the Γ_7 and Γ_5 states that border each other within a classically predicted phase diagram.

The low temperature magnetism of the rare-earth pyrochlore oxides, $R_2B_2O_7$, has become synonymous with complexity and exotic ground states. Both of these are natural consequences of magnetism on the pyrochlore lattice, which is comprised of two site-ordered networks of corner-sharing tetrahedra. This is the canonical three-dimensional crystalline architecture for geometric magnetic frustration, in which competing interactions can preclude or hinder the formation of a classically ordered state. The diversity in the phenomenology of the rare-earth pyrochlores is attributable to the different anisotropies and interactions exhibited by the rare-earth ions that can occupy its magnetic sublattice, which conspire to produce a veritable zoo of magnetic behaviors [1].

A particularly interesting sub-group of the rare-earth pyrochlores are those that exhibit XY spin anisotropy [2], which is obtained when the rare-earth site is occupied by either erbium (Er) or ytterbium (Yb). This XY label is garnered on the basis of their crystal electric field phenomenology, where in both cases, the ground state is an isolated doublet protected by Kramers' theorem, allowing an effective $S = 1/2$ description [3–5]. The anisotropic exchange Hamiltonian, with a form determined by the symmetry of the crystal lattice, provides an appropriate starting point for understanding the ground states of many XY pyrochlores [6–8]. Within the nearest neighbor version of this model, certain sets of exchange parameters can give rise to exotic states such as quantum spin ice [6, 9] or various spin liquids [10, 11], while other sets of exchange parameters are predicted to stabilize classically ordered states [8].

The phase diagram that encompasses the region of parameter space believed to be relevant to the XY pyrochlores contains four distinct $k = 0$ ordered states [8, 15]: ψ_2 non-coplanar antiferromagnet, ψ_3 coplanar antiferromagnet, Γ_7 antiferromagnet (the Palmer-Chalker state [16]), and Γ_9 splayed ferromagnet. Of these states, all but Γ_7 have been experimentally observed in the XY pyrochlores. This XY family is made up of $Yb_2B_2O_7$ and $Er_2B_2O_7$ with B = Ge, Ti, and Sn, where: (i) The order-by-disorder candidate $Er_2Ti_2O_7$ orders into ψ_2 [17] (ii) $Er_2Ge_2O_7$ and $Yb_2Ge_2O_7$ have as-of-yet unidentified ordered states within Γ_5 (ψ_2 or ψ_3) [12, 18] and (iii) Both $Yb_2Sn_2O_7$ [19, 20] and some samples of $Yb_2Ti_2O_7$ [21–25] order into the Γ_9 splayed ferromagnetic state. This ensemble of magnetic ground states supports the picture of a rich phase space.

In this Letter, we present a comprehensive neutron scattering study of $Er_2Pt_2O_7$, a recent addition to the XY family of pyrochlores [5, 14]. Through magnetic symmetry analysis, we find that $Er_2Pt_2O_7$ orders into the Γ_7 Palmer-Chalker state. The Néel ordering temperature, $T_N = 0.38$ K, is a 75% reduction from those of its closest sister pyrochlore antiferromagnets: $Er_2Ti_2O_7$ and $Er_2Ge_2O_7$. Given that the lattice parameter of $Er_2Pt_2O_7$ differs by less then 0.5% from its titanate analog, it is surprising that the transition temperature is so substantially reduced. This dramatic reduction in T_N occurs despite minimal structural modifications and a larger Curie-Weiss temperature, as given in Figure 1. Our inelastic neutron

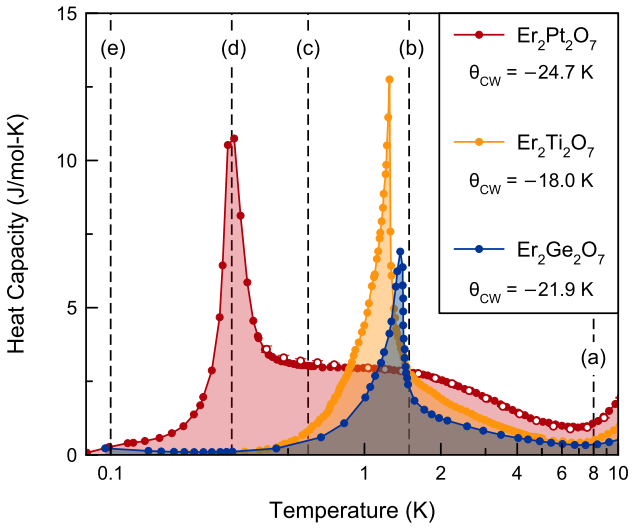

FIG. 1. Low temperature heat capacity of the three sister XY antiferromagnets: $Er_2Ge_2O_7$ [12], $Er_2Ti_2O_7$ [13], and $Er_2Pt_2O_7$, filled in circles from [14] and open circles from our study. The latter two samples magnetically order with $T_N = 1.4$ K and 1.2 K, respectively. In this temperature range, $Er_2Pt_2O_7$ exhibits a broad heat capacity anomaly centered at $T^* = 1.5$ K with a strongly suppressed T_N. The vertical dashed lines indicate the temperatures that correspond with the inelastic scattering spectra that are presented in Figure 3.

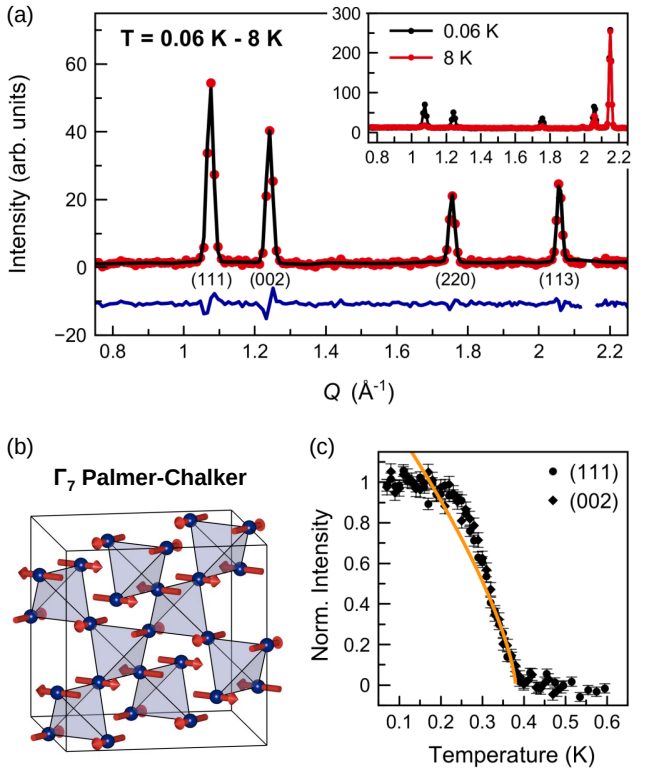

FIG. 2. Rietveld refinement of $Er_2Pt_2O_7$ at 0.06 K, where the magnetic scattering has been isolated by subtracting the 8 K data set. The data (red points) is refined against the Γ_7 magnetic structure, the resulting fit is given by the black curve and the residual is given by the blue curve. The inset shows the unsubtracted elastic scattering at 0.06 K and 8 K. (b) The spin configuration of $Er_2Pt_2O_7$ in its Palmer-Chalker (Γ_7) ground state. (c) The intensity of the (111) and (002) magnetic Bragg peaks as a function of temperature normalized by the average high and low temperature values. A power law fit, given by the yellow curve, gives a critical exponent of $\beta = 0.35 \pm 0.03$.

scattering measurements reveal that strong quasi-elastic spin fluctuations develop in $Er_2Pt_2O_7$ at a temperature well-above T_N, around $T^* = 1.5$ K. This is coincident with the T_N's of both $Er_2Ti_2O_7$ and $Er_2Ge_2O_7$, and a broad peak in its own magnetic heat capacity, as shown in Figure 1. Below $T_N = 0.38$ K, $Er_2Pt_2O_7$'s spin wave spectrum contains a narrow band of low energy spin excitations that are gapped by 0.18 ± 0.02 meV from the elastic position and a diffusive band at higher energy. Spin wave calculations show that the spin excitation spectrum of $Er_2Pt_2O_7$ should contain dispersive higher energy branches that are strikingly absent from the experimental data. We conclude that the origin of the suppressed T_N and the unusual spin dynamics is strong phase competition between the Γ_7 and Γ_5 states.

$Er_2Pt_2O_7$ can be synthesized in the cubic $Fd\bar{3}m$ pyrochlore structure, in powder form only, using high-pressure techniques. We investigated the low temperature magnetic state of our 1.2 gram sample of $Er_2Pt_2O_7$ using both elastic and inelastic neutron scattering techniques. Elastic measurements were performed on the cold neutron triple-axis spectrometer SPINS and time-of-flight inelastic measurements were performed on the Disc Chopper Spectrometer [26], both located at the National Institute for Standards and Technology's Center for Neutron Research. Further details of the synthesis and experimental methods can be found in the Supplemental Material [27].

The magnetically ordered state of $Er_2Pt_2O_7$ can be characterized by the Bragg scattering, which we isolate by integrating over the elastic channel (± 0.05 meV) in the time-of-flight data. As shown in the inset to Figure 2(a), additional Bragg scattering forms upon cooling from 8 K to 0.06 K due to long range magnetic ordering. These magnetic Bragg peaks are resolution limited, corresponding to a minimum correlation length of 132 ± 9 Å. A new Bragg reflection is observed to form on the (002) position, as well as enhanced intensity on the (111), (220), and (113) positions. These magnetic reflections can all be indexed with the propagation vector $k = 0$. The possible $k = 0$ magnetic structures for Er^{3+} at the 16d crystallographic position in the $Fd\bar{3}m$ space group are described by four irreducible representations: $\Gamma_{\rm mag} = \Gamma_3^1 + \Gamma_5^2 + \Gamma_7^3 + \Gamma_9^6$, where the superscript denotes the number of basis vectors for the given representation, which are labeled $\psi_1, \psi_2, ...\psi_{12}$ [28]. Both Γ_3 and Γ_5 can be immediately ruled out, as the (002) magnetic reflection is symmetry forbidden in both of these representations, while (002) is very intense in our

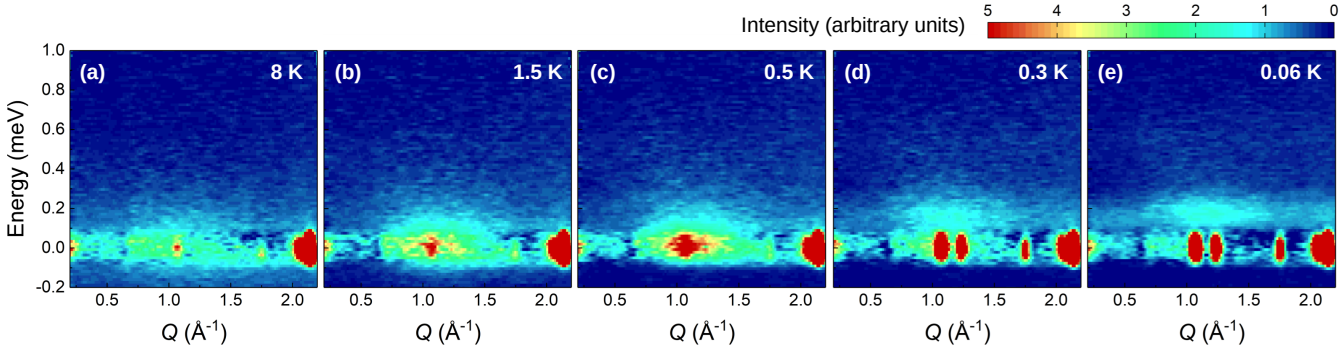

FIG. 3. The inelastic neutron scattering spectra for $Er_2Pt_2O_7$ at (a) 8 K, (b) 1.5 K, (c) 0.5 K, (d) 0.3 K, and (e) 0.06 K. Each data set has had an empty sample can background subtracted. At $T^* = 1.5$ K, the center of the broad specific heat anomaly, short range correlations are building up at 1.1 $Å^{-1}$; these correlations grow more intense down to 0.5 K. Below $T_N = 0.38$ K, the spectral weight segregates into magnetic Bragg peaks and a gapped spin wave excitation.

measured pattern. Furthermore, bulk characterization indicates the ordered state of $Er_2Pt_2O_7$ is antiferromagnetic [14], and Γ_9 is ferromagnetic. Thus, on qualitative grounds alone, one could deduce that $Er_2Pt_2O_7$ orders into the Γ_7 irreducible representation.

To definitively determine the ordered state of $Er_2Pt_2O_7$, we have performed a Rietveld refinement, the result of which is shown in Figure 2(a). The magnetic Bragg scattering was isolated by subtracting a high temperature, 8 K, data set from the 0.06 K data set. All structural and instrumental parameters were fixed according to a refinement of the 8 K data set. Thus, the only parameter allowed to vary for the magnetic refinement at 0.06 K is the size of the ordered moment. Magnetic refinements were attempted with each of the $k = 0$ representations, and the best agreement, $\chi^2 = 2.22$, was obtained with Γ_7, validating our earlier qualitative assessment. Fixing the scale of the magnetic scattering according to the structural component allows us to determine the size of the ordered moment, which is 3.4(2) μ_B at 0.06 K. This ordered moment is approximately 90% of the total moment that was recently determined for the crystal field ground state of $Er_2Pt_2O_7$, $\mu_{CEF} = 3.9$ μ_B [5]. The normalized intensity of the (111) and (002) Bragg peaks as a function of temperature are plotted in Figure 2(c). Fitting a narrow temperature range below $T_N = 0.38$ K to a power law gives the critical exponent $\beta = 0.35 \pm 0.03$, consistent with conventional 3D XY universality [29].

In the Γ_7 ordered state of $Er_2Pt_2O_7$, all spins lie in the plane perpendicular to the local $\langle 111 \rangle$ axes, that connect the vertices of a tetrahedron to its center. The three basis vectors in the Γ_7 manifold are denoted as ψ_4, ψ_5, and ψ_6. These three basis vectors are connected by cubic symmetry transformations, meaning that they are necessarily degenerate and that an equiprobable distribution of all domains will be present in zero magnetic field. Thus, we can arbitrarily proceed by visualizing ψ_4, which is pictured in Figure 2(b). On each tetrahedron, there are two pairs of anti-parallel oriented spins, and all spins are aligned parallel to one of the tetrahedron's edges.

In Figure 3 we present the inelastic neutron scattering spectra for $Er_2Pt_2O_7$ at 8 K, 1.5 K, 0.5 K, 0.3 K and 0.06 K. These temperatures span the range of both specific heat anomalies displayed by $Er_2Pt_2O_7$ and are indicated by the dashed vertical lines in Figure 1. Each of these data sets has had an empty sample can background subtracted from it. We can associate the broad specific heat anomaly at $T^* = 1.5$ K to short range quasi-elastic spin fluctuations, giving rise to a diffuse feature centered at 1.1 $Å^{-1}$. These short range correlations grow more intense upon cooling to 0.5 K. The majority of the diffuse scattering at these temperatures, above T_N, is elastic within our 0.09 meV resolution.

As $Er_2Pt_2O_7$ is cooled through its Néel ordering transition at $T_N = 0.38$ K the diffuse scattering segregates into sharp magnetic Bragg reflections, a narrow inelastic mode centered near 0.2 meV, and a higher energy broad distribution of spin excitations. The upper broad band of excitations is centered at 0.6 meV as can be seen by integrating over our full Q range, as presented in Figure 5(a). However, this upper band of scattering lacks apparent structure as seen in Figure 3(e). The lower band of spin excitations is gapped from the nlastic line by 0.18 ± 0.02 meV. This gap is essentially constant at all wave-vectors, due to the fact that the band itself is so narrow in energy, with a bandwidth of only 0.1 meV. A dispersionless band of excitations, such as this, has been observed in a number of highly frustrated magnetic systems: for example, the "weathervane mode" predicted for two-dimensional Kagome systems [30], and observed in $KFe_3(OH)_6(SO_4)_2$ [31], as well as the singlet-triplet excitations of the frustrated Shastry-Sutherland system, $SrCu_2(BO_3)_2$ [32].

We have performed classical spin wave calculations to further investigate the spin excitations of $Er_2Pt_2O_7$. The powder averaged spin wave spectra were calculated using

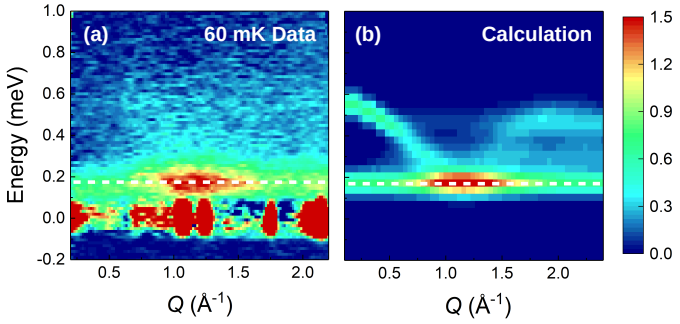

FIG. 4. Comparison of the (a) measured spin wave spectrum of $Er_2Pt_2O_7$ at 60 mK with the (b) calculated spin wave spectrum with $J_1 = 0.10 \pm 0.05$, $J_2 = 0.20 \pm 0.05$, $J_3 = -0.10 \pm 0.03$, and $J_4 = 0$ meV. The calculation captures the lower flat band, indicated by the white dashed line, but predicts a dispersive higher energy mode absent in the measurement.

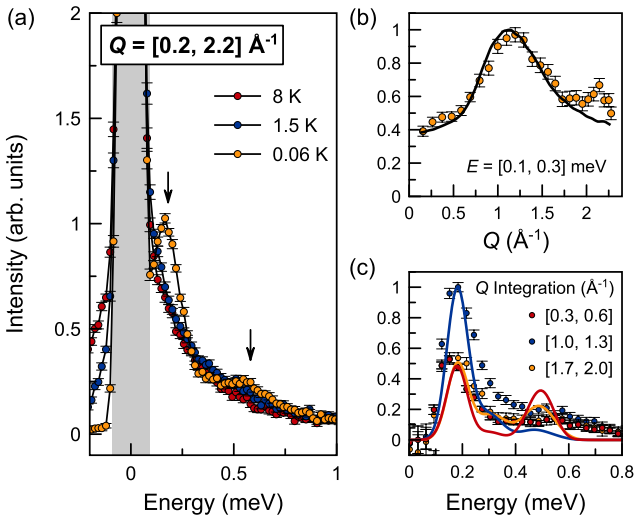

FIG. 5. Integrated scattered intensity of $Er_2Pt_2O_7$ as a function of energy transfer over the full measured Q range, from 0.2 Å^{-1} to 2.2 Å^{-1}. The gray shaded region indicates the elastic resolution. Below T_N, at 0.06 K, the spin excitations are gapped by 0.18 ± 0.02 meV and a weak second band is observed at 0.6 meV. (b) The Q dependence of the lower flat band at $T = 0.06$ K, showing good agreement with the spin wave calculation given by the solid line. (c) Integrations over several representative Q intervals. The spin wave calculation provides a good fit to the flat lower band but predicts a second intense branch not observed in the experimental data.

the anisotropic exchange Hamiltonian [6, 8] and further details can be found in the Supplemental Material [27]. We used the experimentally derived exchange parameters for $Er_2Ti_2O_7$ as an approximate starting point: $J_1 = 0.10$, $J_2 = -0.06$, $J_3 = -0.10$, and $J_4 = 0$ meV [7]. From these values, we carried out a least squares refinement and the best agreement with our experimental spectra for $Er_2Pt_2O_7$ occurs with $J_1 = 0.10 \pm 0.05$, $J_2 = 0.20 \pm 0.05$, $J_3 = -0.10 \pm 0.03$, and $J_4 = 0$ meV. The calculated spin wave spectrum for this set of parameters is presented in Figure 4, where it is presented side-by-side with the lowest temperature experimental data set. This calculated spectra provides a very good description of the low energy flat band, as can be further appreciated by the integrations presented in Figures 5(b) and (c). However, there is a striking discrepancy at higher energies: the computed spin excitation spectrum contains an intense, dispersive mode that is not observed in the experimental data (Fig. 4(a) and 5(c)). It is important to emphasize that this intense, dispersive upper band is present in the computed spectra for the entire range of exchange parameters considered in our study. As our exchange parameters for $Er_2Pt_2O_7$ place it relatively close to the phase boundary between Γ_5 and Γ_7, it is possible that enhanced quantum fluctuations due to phase competition are responsible for the breakdown of the quasiparticles associated with this spin wave branch. Similar phenomenology has recently been investigated in $Yb_2Ti_2O_7$ [33]. Fruitful comparisons can also be made with $Gd_2Sn_2O_7$, which also possesses a Palmer-Chalker ground state below $T_N = 1$ K [28] but with Heisenberg spins rather than XY anisotropy. In addition to a sharp flat band at low energy, the spin wave spectrum of $Gd_2Sn_2O_7$ contains at least two additional sharp branches at higher energies [34]. Thus the breakdown of this upper spin wave branch is not a generic attribute of Palmer-Chalker magnets, evidencing that $Er_2Pt_2O_7$ experiences stronger quantum effects.

The ensemble of $Er_2Pt_2O_7$'s ground state magnetic properties are remarkable, given that it is structurally so similar to $Er_2Ti_2O_7$. Indeed the lattice parameters of these two sister compounds differ by less than 0.5%, far smaller than the 2% difference with the third sister, $Er_2Ge_2O_7$, whose magnetic properties are largely unchanged from $Er_2Ti_2O_7$ [12, 35]. Comparing $Er_2Pt_2O_7$ and $Er_2Ti_2O_7$, we find its Néel ordering temperature is reduced by a factor of three, from 1.2 K to 0.38 K, and the ordered state itself is altered from Γ_5 to Γ_7. Moreover, the spin wave gap of 0.18 ± 0.02 meV is more than triple the 0.053 ± 0.006 meV order-by-disorder spin wave gap observed in $Er_2Ti_2O_7$ [36]. Despite the lower band being very narrow, the full bandwidth of the inelastic scattering in $Er_2Pt_2O_7$, 0.6 meV, is still considerably larger than that of $Er_2Ti_2O_7$, 0.4 meV [37]. Such observations eliminate simple energetic arguments for $Er_2Pt_2O_7$'s anomalously low T_N. Two considerations are important to understand these surprising differences: (i) The partially occupied platinum $5d$ orbital can facilitate superexchange pathways that are inaccessible in closed shell titanium [14, 38], and (ii) The XY pyrochlores live in a rich phase space where modest changes in anisotropic exchange parameters can have a large effect on ground state selection [8]. Indeed, this paradigm predicts that proximity to competing classical phases should manifest as a suppressed ordering temperature [8]. Thus, our observations strongly implicate that $Er_2Pt_2O_7$ resides in a region of exchange

parameter space where it is subject to strong Γ_5-Γ_7 phase competition.

Related phenomenology has previously been observed in the ytterbium family of pyrochlores, including both broad and sharp specific heat anomalies, where the spin dynamics develop well-above T_N or T_C [23, 39–42]. However, for the ytterbium pyrochlores, this competition is between the ferromagnetic Γ_9 state and the antiferromagnetic Γ_5 state [8, 41, 43]. In the case of $Er_2Pt_2O_7$, it is two antiferromagnetic states, Γ_5 and Γ_7, that compete. Thus, we interpret the short-range order at T^* as originating in the spins fluctuating between these two XY states, without breaking the continuous U(1) degeneracy. Then at a lower temperature, T_N, a single manifold is uniquely selected. Conversely, no such broad anomaly or unusual spin dynamics are observed in $Er_2Ti_2O_7$ [37], which orders at a much higher temperature and for which phase competition is certainly less important [8].

We have shown that $Er_2Pt_2O_7$ is an XY pyrochlore that realizes a Palmer-Chalker (Γ_7) ground state, with $T_N = 0.38$ K and an ordered moment of 3.4(2) μ_B. The spin dynamics develop well-above the ordering temperature, near $T^* = 1.5$ K, the origin of the broad specific anomaly. The dramatically suppressed ordering temperature and change of ground state in $Er_2Pt_2O_7$ can be understood in the context of strong phase competition. Multiphase competition is already understood to be important within the ytterbium family of pyrochlores and our work shows that this premise can equally be expanded into the erbium pyrochlores.

Note added: Following the submission of this paper, a related manuscript on another erbium XY pyrochlore, $Er_2Sn_2O_7$, appeared on the arXiv [44]. This material is also found to possess a Palmer-Chalker ground state with $T_N = 0.1$ K. Evidence is also found for frustration induced by phase competition, consistent with our arguments on its relevance to erbium pyrochlores.

We greatly appreciate the technical support from Juscelino Leao and Yegor Vekhov at the NIST Center for Neutron Research. A.M.H. acknowledges support from the Vanier Canada Graduate Scholarship Program and thanks the National Institute for Materials Science (NIMS) for their hospitality and support through the NIMS Internship Program. This work was supported by the Natural Sciences and Engineering Research Council of Canada. We acknowledge the support of the National Institute of Standards and Technology, U.S. Department of Commerce, in providing the neutron research facilities used in this work. Identification of commercial equipment does not imply endorsement by NIST. C.R.W. acknowledges CFI and the CRC program (Tier II).

[1] J. S. Gardner, M. J. P. Gingras, and J. E. Greedan, Rev. Mod. Phys. **82**, 53 (2010).
[2] A. M. Hallas, J. Gaudet, and B. D. Gaulin, to appear in Annu. Rev. Condens. Matter Phys. (2017).
[3] S. Guitteny, S. Petit, E. Lhotel, J. Robert, P. Bonville, A. Forget, and I. Mirebeau, Phys. Rev. B **88**, 134408 (2013).
[4] J. Gaudet, D. D. Maharaj, G. Sala, E. Kermarrec, K. A. Ross, H. A. Dabkowska, A. I. Kolesnikov, G. E. Granroth, and B. D. Gaulin, Phys. Rev. B **92**, 134420 (2015).
[5] J. Gaudet, A. M. Hallas, A. I. Kolesnikov, and B. D. Gaulin, arXiv:1708.01176 (2017).
[6] K. A. Ross, L. Savary, B. D. Gaulin, and L. Balents, Phys. Rev. X **1**, 021002 (2011).
[7] L. Savary, K. A. Ross, B. D. Gaulin, J. P. C. Ruff, and L. Balents, Phys. Rev. Lett. **109**, 167201 (2012).
[8] H. Yan, O. Benton, L. Jaubert, and N. Shannon, Phys. Rev. B **95**, 094422 (2017).
[9] M. J. P. Gingras and P. A. McClarty, Rep. Prog. Phys. **77**, 056501 (2014).
[10] B. Canals and C. Lacroix, Phys. Rev. Lett. **80**, 2933 (1998).
[11] O. Benton, L. D. C. Jaubert, H. Yan, and N. Shannon, Nat. Commun. **7** (2016).
[12] Z. L. Dun, X. Li, R. S. Freitas, E. Arrighi, C. R. Dela Cruz, M. Lee, E. S. Choi, H. B. Cao, H. J. Silverstein, C. R. Wiebe, J. G. Cheng, and H. D. Zhou, Phys. Rev. B **92**, 140407 (2015).
[13] P. D. de Réotier, A. Yaouanc, Y. Chapuis, S. H. Curnoe, B. Grenier, E. Ressouche, C. Marin, J. Lago, C. Baines, and S. R. Giblin, Phys. Rev. B **86**, 104424 (2012).
[14] Y. Q. Cai, Q. Cui, X. Li, Z. L. Dun, J. Ma, C. dela Cruz, Y. Y. Jiao, J. Liao, P. J. Sun, Y. Q. Li, J. S. Zhou, J. B. Goodenough, H. D. Zhou, and J.-G. Cheng, Phys. Rev. B **93**, 014443 (2016).
[15] A. W. C. Wong, Z. Hao, and M. J. P. Gingras, Phys. Rev. B **88**, 144402 (2013).
[16] S. E. Palmer and J. T. Chalker, Phys. Rev. B **62**, 488 (2000).
[17] A. Poole, A. S. Wills, and E. Lelievre-Berna, J. Phys.: Condens. Matter **19**, 452201 (2007).
[18] A. M. Hallas, J. Gaudet, M. N. Wilson, T. J. Munsie, A. A. Aczel, M. B. Stone, R. S. Freitas, A. M. Arevalo-Lopez, J. P. Attfield, M. Tachibana, C. R. Wiebe, G. M. Luke, and B. D. Gaulin, Phys. Rev. B **93**, 104405 (2016).
[19] A. Yaouanc, P. Dalmas de Réotier, P. Bonville, J. A. Hodges, V. Glazkov, L. Keller, V. Sikolenko, M. Bartkowiak, A. Amato, C. Baines, P. J. C. King, P. C. M. Gubbens, and A. Forget, Phys. Rev. Lett. **110**, 127207 (2013).
[20] J. Lago, I. Živković, J. O. Piatek, P. Álvarez, D. Hüvonen, F. L. Pratt, M. Díaz, and T. Rojo, Phys. Rev. B **89**, 024421 (2014).
[21] Y. Yasui, M. Soda, S. Iikubo, M. Ito, M. Sato, N. Hamaguchi, T. Matsushita, N. Wada, T. Takeuchi, N. Aso, and K. Kakurai, J. Phys. Soc. Jpn **72**, 3014 (2003).
[22] L.-J. Chang, S. Onoda, Y. Su, Y.-J. Kao, K.-D. Tsuei, Y. Yasui, K. Kakurai, and M. R. Lees, Nat. Commun. **3**, 992 (2012).
[23] J. Gaudet, K. A. Ross, E. Kermarrec, N. P. Butch, G. Ehlers, H. A. Dabkowska, and B. D. Gaulin, Phys.

Rev. B **93**, 064406 (2016).
[24] A. Yaouanc, P. D. de Réotier, L. Keller, B. Roessli, and A. Forget, J. Phys.: Condens. Matter **28**, 426002 (2016).
[25] A. Scheie, J. Kindervater, S. Säubert, C. Duvinage, C. Pfleiderer, H. J. Changlani, S. Zhang, L. Harriger, S. M. Koohpayeh, O. Tchernyshyov, and C. Broholm, arXiv:1703.06904 (2017).
[26] J. R. D. Copley and J. C. Cook, Chem. Phys. **292**, 477 (2003).
[27] See Supplemental Material [url] for further information on (i) the synthesis and experimental details of the neutron scattering measurements (ii) the order parameter measurements and (iii) details related to the linear spin wave calculations, which includes Refs. [45–54].
[28] A. S. Wills, M. E. Zhitomirsky, B. Canals, J. P. Sanchez, P. Bonville, P. D. de Réotier, and A. Yaouanc, J. Phys.: Condens. Matter **18**, L37 (2006).
[29] M. Campostrini, M. Hasenbusch, A. Pelissetto, P. Rossi, and E. Vicari, Phys. Rev. B **63**, 214503 (2001).
[30] P. Chandra, P. Coleman, and I. Ritchey, Journal de Physique I **3**, 591 (1993).
[31] K. Matan, D. Grohol, D. G. Nocera, T. Yildirim, A. B. Harris, S. H. Lee, S. E. Nagler, and Y. S. Lee, Phys. Rev. Lett. **96**, 247201 (2006).
[32] B. D. Gaulin, S. H. Lee, S. Haravifard, J. P. Castellan, A. J. Berlinsky, H. A. Dabkowska, Y. Qiu, and J. R. D. Copley, Phys. Rev. Lett. **93**, 267202 (2004).
[33] J. D. Thompson, P. A. McClarty, D. Prabhakaran, I. Cabrera, T. Guidi, and R. Coldea, Phys. Rev. Lett. **119**, 057203 (2017).
[34] J. R. Stewart, J. S. Gardner, Y. Qiu, and G. Ehlers, Phys. Rev. B **78**, 132410 (2008).
[35] X. Li, W. M. Li, K. Matsubayashi, Y. Sato, C. Q. Jin, Y. Uwatoko, T. Kawae, A. M. Hallas, C. R. Wiebe, A. M. Arevalo-Lopez, J. P. Attfield, J. S. Gardner, R. S. Freitas, H. D. Zhou, and J.-G. Cheng, Phys. Rev. B **89**, 064409 (2014).
[36] K. A. Ross, Y. Qiu, J. R. D. Copley, H. A. Dabkowska, and B. D. Gaulin, Phys. Rev. Lett. **112**, 057201 (2014).
[37] J. P. C. Ruff, J. P. Clancy, A. Bourque, M. A. White, M. Ramazanoglu, J. S. Gardner, Y. Qiu, J. R. D. Copley, M. B. Johnson, H. A. Dabkowska, and B. D. Gaulin, Phys. Rev. Lett. **101**, 147205 (2008).
[38] A. M. Hallas, A. Z. Sharma, Y. Cai, T. J. Munsie, M. N. Wilson, M. Tachibana, C. R. Wiebe, and G. M. Luke, Phys. Rev. B **94**, 134417 (2016).
[39] K. A. Ross, J. P. C. Ruff, C. P. Adams, J. S. Gardner, H. A. Dabkowska, Y. Qiu, J. R. D. Copley, and B. D. Gaulin, Phys. Rev. Lett. **103**, 227202 (2009).
[40] Z. L. Dun, E. S. Choi, H. D. Zhou, A. M. Hallas, H. J. Silverstein, Y. Qiu, J. R. D. Copley, J. S. Gardner, and C. R. Wiebe, Phys. Rev. B **87**, 134408 (2013).
[41] J. Robert, E. Lhotel, G. Remenyi, S. Sahling, I. Mirebeau, C. Decorse, B. Canals, and S. Petit, Phys. Rev. B **92**, 064425 (2015).
[42] A. M. Hallas, J. Gaudet, N. P. Butch, M. Tachibana, R. S. Freitas, G. M. Luke, C. R. Wiebe, and B. D. Gaulin, Phys. Rev. B **93**, 100403 (2016).
[43] L. D. C. Jaubert, O. Benton, J. G. Rau, J. Oitmaa, R. R. P. Singh, N. Shannon, and M. J. P. Gingras, Phys. Rev. Lett. **115**, 267208 (2015).
[44] S. Petit, E. Lhotel, F. Damay, P. Boutrouille, A. Forget, and D. Colson, arXiv:1705.04462 (2017).
[45] C. R. Wiebe and A. M. Hallas, APL Materials **3**, 041519 (2015).
[46] A. M. Hallas, A. M. Arevalo-Lopez, A. Z. Sharma, T. Munsie, J. P. Attfield, C. R. Wiebe, and G. M. Luke, Phys. Rev. B **91**, 104417 (2015).
[47] H. R. Hoekstra and F. Gallagher, Inorg. Chem. **7**, 2553 (1968).
[48] A. W. Sleight, Mater. Res. Bull. **3**, 699 (1968).
[49] R. T. Azuah, L. R. Kneller, Y. Qiu, P. L. Tregenna-Piggott, C. M. Brown, J. R. D. Copley, and R. M. Dimeo, J. Res. Natl. Inst. Stand. Technol. **114**, 341 (2009).
[50] A. S. Wills, Phys B **276**, 680 (2000).
[51] J. Rodríguez-Carvajal, Phys B **192**, 55 (1993).
[52] J. D. M. Champion, M. J. Harris, P. C. W. Holdsworth, A. S. Wills, G. Balakrishnan, S. T. Bramwell, E. Čižmár, T. Fennell, J. S. Gardner, J. Lago, D. F. McMorrow, M. Orendáč, A. Orendáčová, D. M. Paul, R. I. Smith, M. T. F. Telling, and A. Wildes, Phys. Rev. B **68**, 020401 (2003).
[53] S. H. Curnoe, Phys. Rev. B **75**, 212404 (2007).
[54] S. Toth and B. Lake, Journal of Physics: Condensed Matter **27**, 166002 (2015).